Transactions of the **13th International Conference on Structural Mechanics in Reactor Technology** (SMiRT 13), Escola de Engenharia - Universidade Federal do Rio Grande do Sul, Porto Alegre, Brazil, August 13-18, 1995

Forced vibration test of the Hualien large scale SSI model (part 2)

Sugawara, Y.[1], Uetake, T.[1], Kobayashi, T.[2], Yamaya, H.[2]
1) Tokyo Eletric Power Company, Tokyo, Japan
2) Kajima Technical Research Institute, Tokyo, Japan

ABSTRACT: A Large-Scale Seismic Test (LSST) Program conducted at Hualien (stiff soil site), Taiwan, has started[1)] to obtain earthquake-induced soil-structure interaction (SSI) data as an extension of the same kind of program conducted at Lotung (soft soil site). Two tests have been performed: a Forced Vibration Test (FVT) without embedment[4)] and the same test with embedment. Horizontal excitations were applied in two different directions both on the roof slab and on the basemat of a 1/4-scale containment model. Vertical excitations were applied on the basemat only.

The concept of "Principal Axes (D_1, D_2)" was introduced for the SSI system, and the basic dynamic characteristics of the soil-structure system were obtained for D_1 and D_2. As an example, peak frequencies for horizontal excitation were 4.1 and 4.6 Hz without embedment, and 6.1 and 6.3 Hz with embedment for D_1 and D_2 based on results transformed to principal axes. Finally, a soil impedance function was obtained by a newly defined error minimizing method. This function also simulates the classic embedment effect.

1 INTRODUCTION

The Hualien program was started to obtain earthquake-induced soil-structure interaction data in order to study soil-structure interaction effects, using a 1/4-scale reinforced cylindrical concrete containment model constructed at Hualien, Taiwan.

Before starting earthquake observations, forced vibration tests were conducted to obtain basic dynamic characteristics of the soil-structure interaction system.

The resonance curves without embedment for both NS and EW excitation tests had two peaks. Furthermore, it was clarified that soil inhomogeneity existed in a direction 34° counterclockwise from the NS direction.

This paper discusses the results of the second phase of forced vibration tests (FVT-2) with embedment and its analysis method. The first phase of FVT (without embedment) is called FVT-1.

Details of the tested model were described in the last paper [4)]. A section of the model structure is shown in Fig. 1.

2 GEOTECHNICAL INVESTIGATION

During the vibration tests, soil inhomogeneity was observed by sight. After forced vibration tests without embedment, a geotechnical soil investigation was carried out [5)]. Based on its results, the inhomogeneity suggested in the last paper was established.

Fig. 2 shows the results of a soil investigation in the range of 1 m below the foundation. According to these data, the shear wave velocity (V_s) of one quarter of this depth was over 300 m/sec, but that of the other three quarters was under 300 m/sec. This distribution of shear wave velocity caused the existence of principal axes.

3 TEST RESULTS

Fig. 3 shows the horizontal displacement resonance curves and phase lag curves for NS and EW direction excitations at the roof. The resonance curve for the NS direction excitation had a peak at 6.1 Hz, and that for the EW direction excitation had a peak at 6.3 Hz. The response amplitudes with embedment were 1/4 of those without embedment, and they had a single peak. Fig. 4 shows the vibration mode shapes at the peak frequencies. The component orthogonal to the excitation direction was about 20 % of that in the excitation direction. This result indicates that the resonance displacement orbit for each excitation direction is elliptical, as it is without embedment.

Fig. 5 shows the response displacement orbit for the NS and EW excitations at the roof. Each orbit is elliptical. This means that the orthogonal component has a significant phase lag.

The angle of the principal axis was determined as 34° by trial and error in the last paper. In the present study, an eigen value analysis for a variance-covariance matrix was performed. In this case, the arc tangent is given as an angle of the long axis of the response orbit. As a result, the angle of principal axis is obtained as 34° without embedment and 30° with embedment.

The orbit for the combined the principal direction excitation after transformation is shown in Fig. 6. As shown, each orbit is a straight line and no orthogonal component appears. This indicates that direction D_1 and D_2 response components are not combined for direction D_1 and D_2 excitations. Fig. 7 shows the horizontal displacement resonance curves and the phase lag curves for the principal axis excitations at the roof. Each resonance curve has a single peak and orthogonal components are negligible.

Based on these transformed results, fundamental frequencies and damping factors are obtained. Furthermore, the ratios of displacement components (sway, rocking and elastic deformation of the structure) at the roof floor in the fundamental mode shapes are obtained as shown in Table 1. This table also includes results without embedment as FVT-1. The fundamental frequencies are about 6.1 Hz for D_1 and 6.3 Hz for D_2, and the damping factors are about 8% for both directions with embedment.

The ratio of sway in the displacement at the roof with embedment is less than 10 %, which is about half of that without embedment, and that of rocking is about 50 % for each excitation level.

4 SOIL IMPEDANCE FUNCTION

Horizontal Displacement $\tilde{u}$ and rotation angle $\tilde{\phi}$ regressed from test results are given as :

$$\begin{Bmatrix} \tilde{u} \\ \tilde{\phi} \end{Bmatrix} = \begin{bmatrix} D_{11} & D_{12} \\ D_{21} & D_{22} \end{bmatrix} \begin{Bmatrix} Q \\ M \end{Bmatrix}$$

where D_{ij} is the flexibility matrix of the soil, and Q and M are the shear force and the moment at the base mat bottom obtained from the test results based on the lumped mass model shown Fig. 8.

To minimize the measured relative error value and regression value at sway, and rocking component of roof floor displacement, a newly defined as error function is

$$\varepsilon^2 = \left(\frac{u_1-\tilde{u}_1}{u_1}\right)^2 + \left(\frac{H\phi_1-H\tilde{\phi}_1}{H\phi_1}\right)^2 + \left(\frac{u_2-\tilde{u}_2}{u_2}\right)^2 + \left(\frac{H\phi_2-H\tilde{\phi}_2}{H\phi_2}\right)^2$$

where subscripts 1 and 2 represent roof floor excitation and first floor excitation, respectively. The compliance matrix for soil can be calculated as an inversion of the obtained flexibility matrix by minimizing error given by the above equation.

$$\begin{bmatrix} K_{HH} & K_{HR} \\ K_{HR} & K_{RR} \end{bmatrix} = \begin{bmatrix} D_{11} & D_{12} \\ D_{21} & D_{22} \end{bmatrix}^{-1}$$

where K_{ij}: Compliance matrix of soil

Fig. 9 shows the obtained soil impedance function for D_1 and D_2, respectively. According to these data, embedment effect is confirmed, because the value of both the real and the imaginary part of soil impedance with embedment function are greater than those without embedment around the peak frequency in both direction. It is recognized that backfill (embedment) soil contributed to radiation damping.

5 CONCLUSIONS

From the tests and analysis, the following conclusions are obtained:

1. The dynamic characteristics of the soil-structure interaction system are not axi-symmetric and have a principal axis 34° counterclockwise from the NS direction without embedment and 30° with embedment.
2. The soil-structure interaction system is not axi-symmetric because of the soil inhomogeneity. The direction of the principal axis correlates well with that obtained from the site and geotechnical soil investigation.
3. The basic dynamic characteristics of the soil-structure system with and without embedment, e. g. , natural frequencies, damping factors and mode shapes, are obtained for the principal axis.
4. Soil impedances were derived from the test results using the newly defined method of minimizing the error function. As a result, classic embedment effects were observed.

REFERENCE

1) Tang, H. T. et al. 1991. The Hualien Large-Scale Seismic Test for Soil-Structure Interaction Research. *Proc. 11-SMiRT*, K04/4, Tokyo, Japan.
2) Tang, H. T. 1987. Large-Scale Soil-Structure Interaction. EPRI NP-5513-SR.
3) EPRI. 1989. *Proc. EPRI/NRC/TPC Workshop on Seismic Soil-Structure Interaction Analysis Techniques Using Data From Lotung, Taiwan*, Volumes 1 and 2. EPRI NP-6154.
4) H. MORISHITA et al. 1993. Forced Vibration Test of the Hualien Large Scale SSI Model. *Proc. 12-SMiRT*, K02/1, Stuttgart, Germany.
5) T. Kokusho et al. 1993. Geotechnical Investigation in the Hualien Large Scale Seismic Test Project, *Proc. 12-SMiRT* , K03/4, Stuttgart, Germany.

Table 1 Test Results

					Displacement Ratios(%)		
FVT	Excitation Position	Excitation Direction	Natural Freq. (Hz)	Damping Factor(%)	Sway	Rocking	Super Structure
1	Roof	D_1	4.1	3.6	12	67	21
		D_2	4.6	3.7	12	65	23
	First	D_1	4.2	3.6	14	61	25
		D_2	4.6	3.7	12	66	22
	First	UD	11.0	29.4	(Soil) 83		17
2	Roof	D_1	6.1	8.2	7	52	41
		D_2	6.3	8.2	8	49	43
	First	D_1	6.5	8.6	5	55	40
		D_2	6.6	8.1	6	48	46
	First	UD	10.8	45.4	(Soil) 82		18

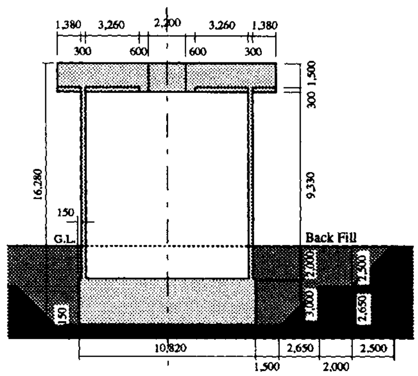

Fig. 1 Cross Section of Model Structure

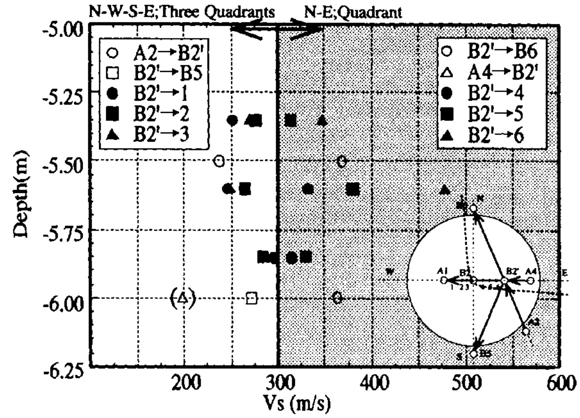

Fig. 2 Geotechnical Investigation Results

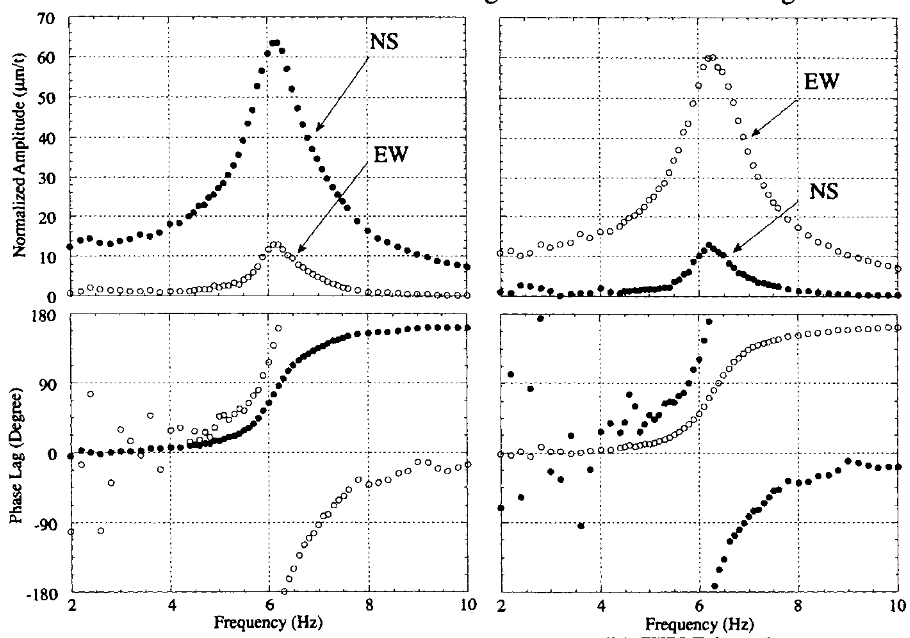

(a) NS Direction (b) EW Direction

Fig. 3 Horizontal Displacement Resonance Curves and Phase Lag Curves for NS and EW Excitation at Roof Floor (with embedment)

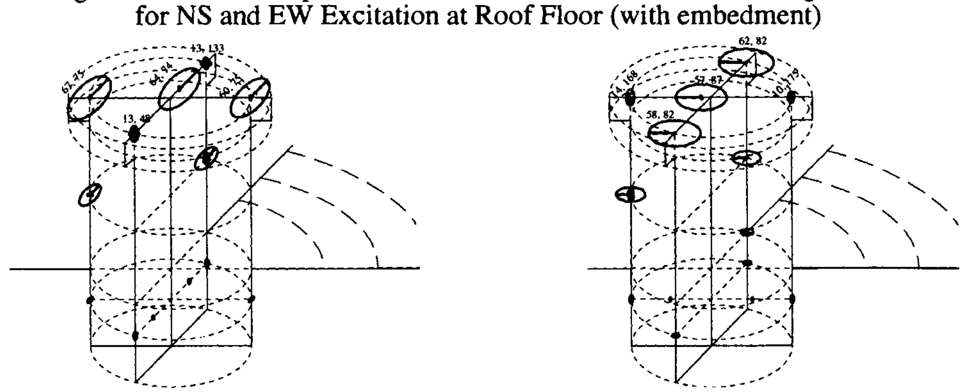

(a) NS Excitation (6.1Hz) (b) EW Excitation (6.3Hz)

Fig.4 Mode Shapes at Peak Frequency (with embedment)

*Number means normalized amplitude(μm/t), Phase Lag (degree).

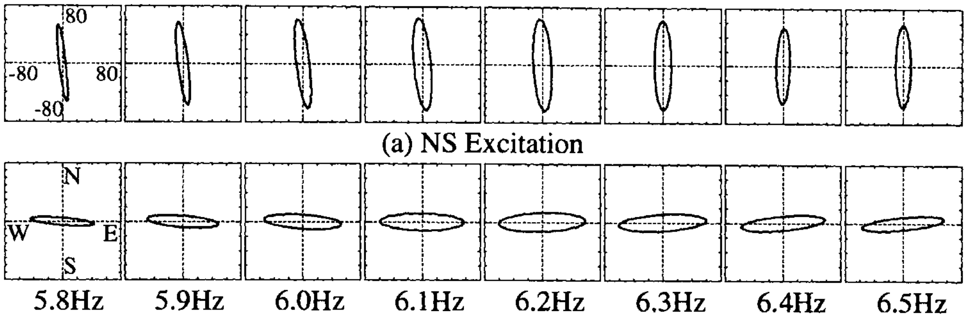

(a) NS Excitation

(b) EW Excitation (Unit: μm/ton)

Fig.5 Orbit of Roof Floor for NS and EW Excitation at Roof (with embedment)

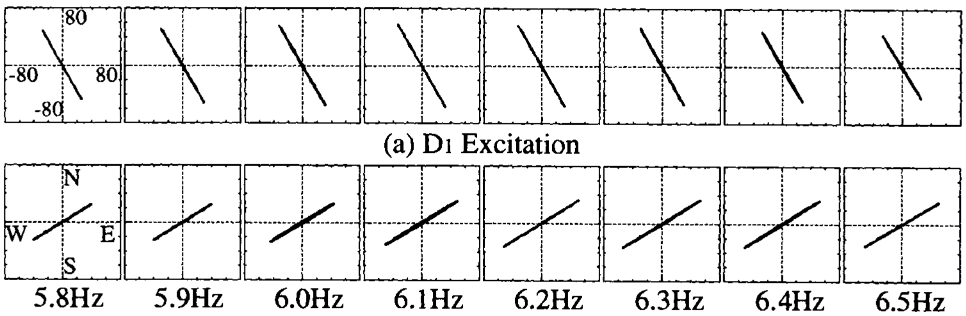

(a) D1 Excitation

(b) D2 Excitation (Unit: μm/ton)

Fig.6 Orbit of Roof Floor for Principal Axis Excitation at Roof (with embedment)

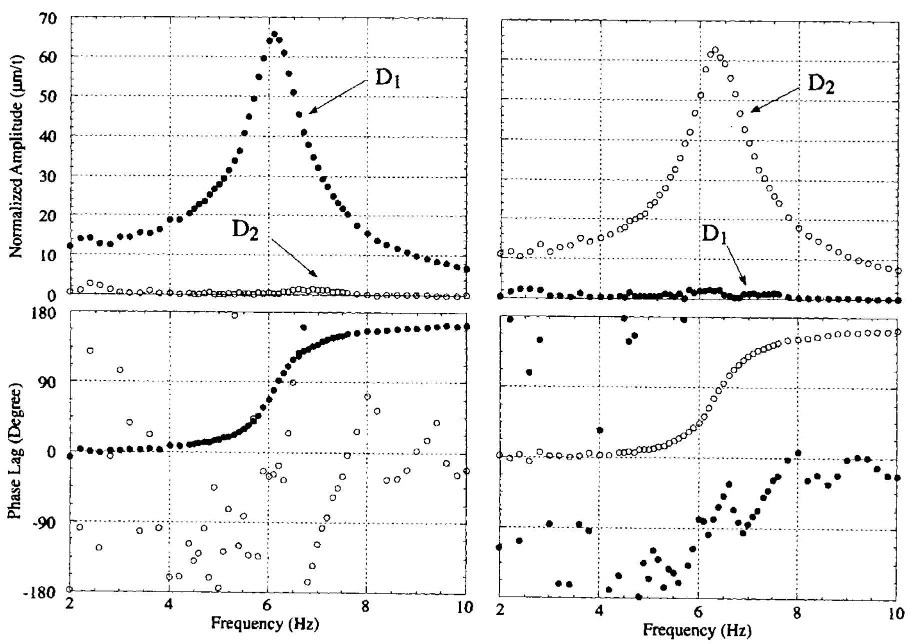

(a) D1 Direction

(b) D2 Direction

Fig. 7 Horizontal Displacement Resonance Curves and Phase Lag Curves for Principal Excitation at Roof Floor (with embedment)

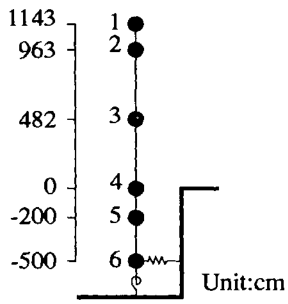

Node No.	Mass Element	
	Weight (tf)	Rotational Inertia ($\times 10^4$ t cm^2)
1	243	2.779
2	324	3.827
3	111	1.672
4	79	1.146
5	354	2.980
6	331	2.670

Fig. 8 Mathematical Model of Structure

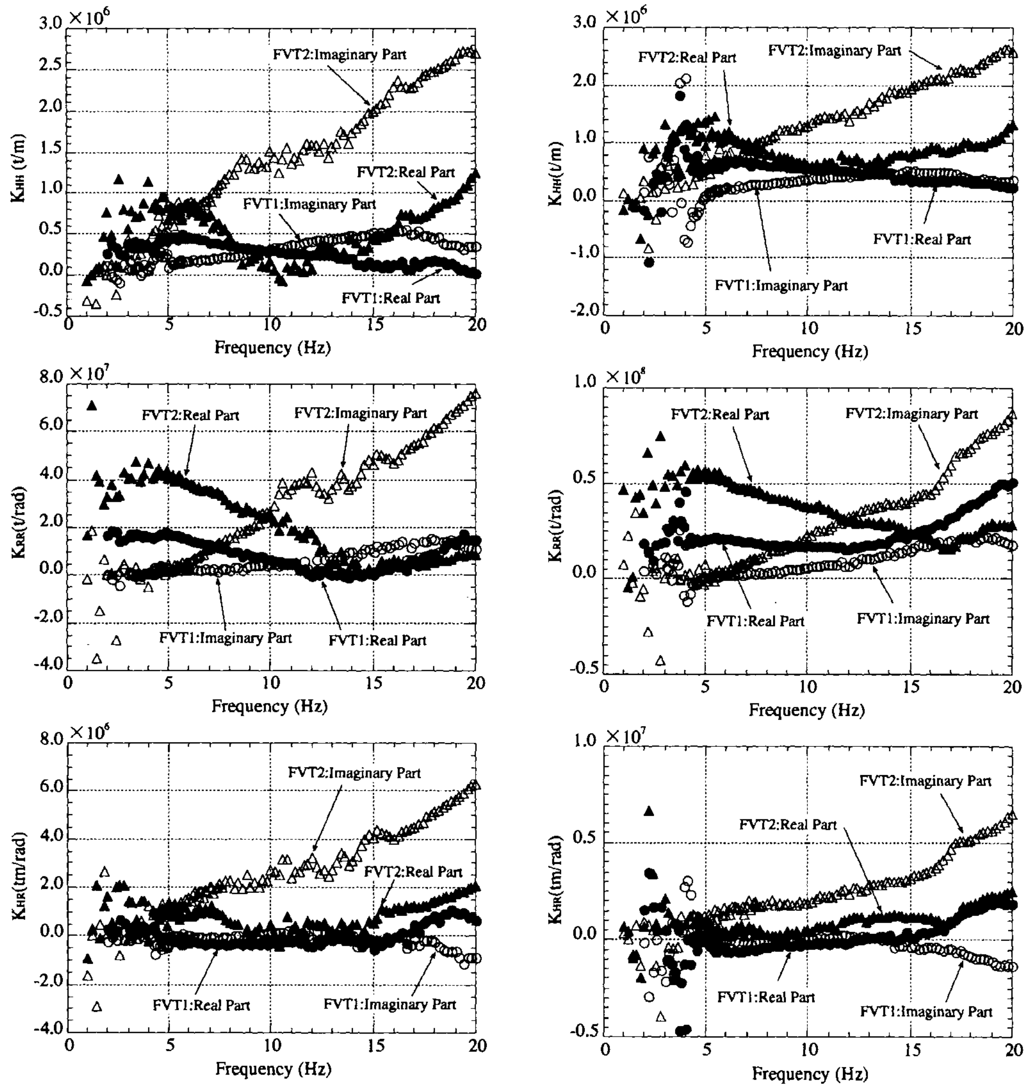

(a) D_1 Direction (b) D_2 Direction

Fig. 9 Soil Impedance